



Canadian Journal of Chemistry  
Revue canadienne de chimie

**An engineered one-site aptamer with higher sensitivity for label-free detection of adenosine on graphene oxide**

Journal:	<i>Canadian Journal of Chemistry</i>
Manuscript ID	cjc-2017-0601.R1
Manuscript Type:	Article
Date Submitted by the Author:	22-Jan-2018
Complete List of Authors:	Zhang, Zijie; University of Waterloo, Chemistry Liu, Juewen; University of Waterloo, Chemistry
Is the invited manuscript for consideration in a Special Issue?:	Emerging Nano/Hybrid Materials
Keyword:	Graphene oxide, Biosensors, Aptamers, Fluorescence

SCHOLARONE™  
Manuscripts

1  
2  
3  
4  
5  
6  
7  
8

**An engineered one-site aptamer with higher sensitivity for label-free  
detection of adenosine on graphene oxide**

Zijie Zhang and Juewen Liu\*

Department of Chemistry, Waterloo Institute for Nanotechnology, University of Waterloo,  
Waterloo, Ontario, N2L 3G1, Canada

Email: liujw@uwaterloo.ca

Draft

## 1 **Abstract**

2 The 27-nucleotide DNA aptamer for adenosine and ATP, originally selected by the Szostak lab  
3 in 1995, has been a very popular model system for biosensor development. This unique aptamer  
4 has two target binding sites and we recently showed that it is possible to remove either site while  
5 the other one still retains binding. From an analytical perspective, tuning the number of binding  
6 sites has important implications in modulating sensitivity of the resulting biosensors. In this work,  
7 we report that the engineered one-site aptamer showed excellent signaling properties with a 2.6-  
8 fold stronger signal intensity and also a 4.2-fold increased detection limit compared to the wild-  
9 type two-site aptamer. The aptamer has a hairpin structure and the length of the hairpin stem was  
10 systematically varied for the one-site aptamers. Isothermal titration calorimetry and a label-free  
11 fluorescence signaling method with graphene oxide and SYBR Green I were respectively used to  
12 evaluate binding and sensor performance. While longer stemmed aptamers produced better  
13 adenosine binding affinity, the signaling was quite independent of the stem length as long as  
14 more than three base pairs were left. This was explained by the higher affinity of binding to GO  
15 by the longer aptamers, cancelling out the higher affinity for adenosine binding. This work  
16 further confirms the analytical applications of such one-site adenosine aptamers, which are  
17 potentially useful for improved ATP imaging and for developing new biosensors.

18

19

## 1 Introduction

2 Aptamers are single-stranded nucleic acids that can selectively bind to target molecules.<sup>1-3</sup> Since  
3 its discovery, aptamers have been widely used for biosensor development.<sup>4-12</sup> Aptamers binding  
4 to small molecules are particularly attractive since they often show even better binding properties  
5 than antibodies.<sup>13,14</sup> The 27-nucleotide DNA aptamer for adenosine, AMP and ATP isolated by  
6 Huizenga and Szostak in 1995 is an extensively studied model aptamer,<sup>15</sup> and it has been used  
7 for measuring ATP in various samples.<sup>16-22</sup> This aptamer is unique in terms of its simultaneous  
8 binding of two target molecules, while very few aptamers for small molecules have such a  
9 property.<sup>23-25</sup>

10 We were quite intrigued by the two binding sites and found that binding was still retained even  
11 when one of the sites was removed.<sup>26</sup> The resulting one-site aptamer could be shorter with even  
12 higher sensitivity since the need of cooperative binding was eliminated. To have a systematic  
13 understanding of its analytical performance, we herein explored a series of one-site aptamers and  
14 made a comparison with the wild-type two-site aptamer. Our goal was to identify the optimal  
15 sensing sequences using a label-free signaling method.

16 Graphene oxide (GO) has been a unique platform for designing DNA-based biosensors in the  
17 past few years.<sup>27-32</sup> GO can adsorb non-structured single-stranded DNA and quench  
18 fluorescence.<sup>33-36</sup> By adding the aptamer target, the equilibrium is shifted towards the aptamer  
19 leaving the surface and increasing fluorescence. GO also allows the development of label-free  
20 sensors by using DNA staining dyes,<sup>37-39</sup> which makes sensor optimization cost-effective. In this  
21 work, we systematically studied the signaling of various engineered adenosine aptamers  
22 adsorbed onto GO, and our results confirmed one-site aptamers were better than the wild-type  
23 two-site aptamer for more sensitive detection.

## 1 **Materials and Methods**

2 **Chemicals.** All the DNA samples were purchased from Integrated DNA Technologies (IDT,  
3 Coralville, IA, USA). Single layer carboxyl graphene oxide (GO) was purchased from ACS  
4 Material (Medford, MA). Sodium chloride, magnesium chloride, 4-(2-hydroxyethyl)-1-  
5 piperazineethanesulfonic acid (HEPES), adenosine, other nucleosides and nucleotides were from  
6 Mandel Scientific (Guelph, ON, Canada). Fetal bovine serum (FBS) was purchased from Sigma-  
7 Aldrich (St Louis, USA). 10000× SYBR Green I dye in dimethyl sulfoxide (DMSO) was  
8 purchased from Invitrogen (Carlsbad, CA). Milli-Q water was used to prepare all the buffers and  
9 solutions.

10 **ITC.** Isothermal titration calorimetry (ITC) was performed using a VP-ITC microcalorimeter  
11 instrument (MicroCal). All the ITC tests used the following protocols unless otherwise specified.  
12 Prior to each measurement, each solution was degassed to remove air bubbles. An aptamer  
13 sample (10 μM) in buffer A (20 mM HEPES, pH 7.6, NaCl 100 mM and 2 mM MgCl<sub>2</sub>) was  
14 loaded in a 1.45 ml ITC cell at 15 °C. Adenosine or other nucleosides (280 μL, 0.5mM) in the  
15 same buffer were titrated into the cell through a syringe (10 μL each time, except for the first  
16 injection of 2 μL). The enthalpy ( $\Delta H$ ) and binding constant ( $K_a$ ) were obtained through fitting the  
17 titration curves to a one-site binding model using the Origin software. The dissociation constant  
18 ( $K_d$ ) values were calculated from  $1/K_a$  and  $\Delta G = -RT \ln(K_a)$ , where  $R$  is the gas constant.  $\Delta S$  was  
19 calculated from  $\Delta G = \Delta H - T\Delta S$ .

20 **DLS and TEM.** The hydrodynamic size and  $\zeta$ -potential of GO (50 μg/mL) was measured using  
21 dynamic light scattering (DLS) on a Malvern Zetasizer Nano ZS90 with a He-Ne laser (633 nm)  
22 at 90° collecting optics at 25 °C in the buffer A. Transmission electron microscopy (TEM) was  
23 performed on a Philips CM10 transmission electron microscope with an acceleration voltage of

1 80 kV. The sample was prepared by pipetting a drop of the GO aqueous dispersion (100  $\mu\text{g}/\text{mL}$ )  
2 onto a 230 mesh copper holey carbon grid and then dried in air for tests.

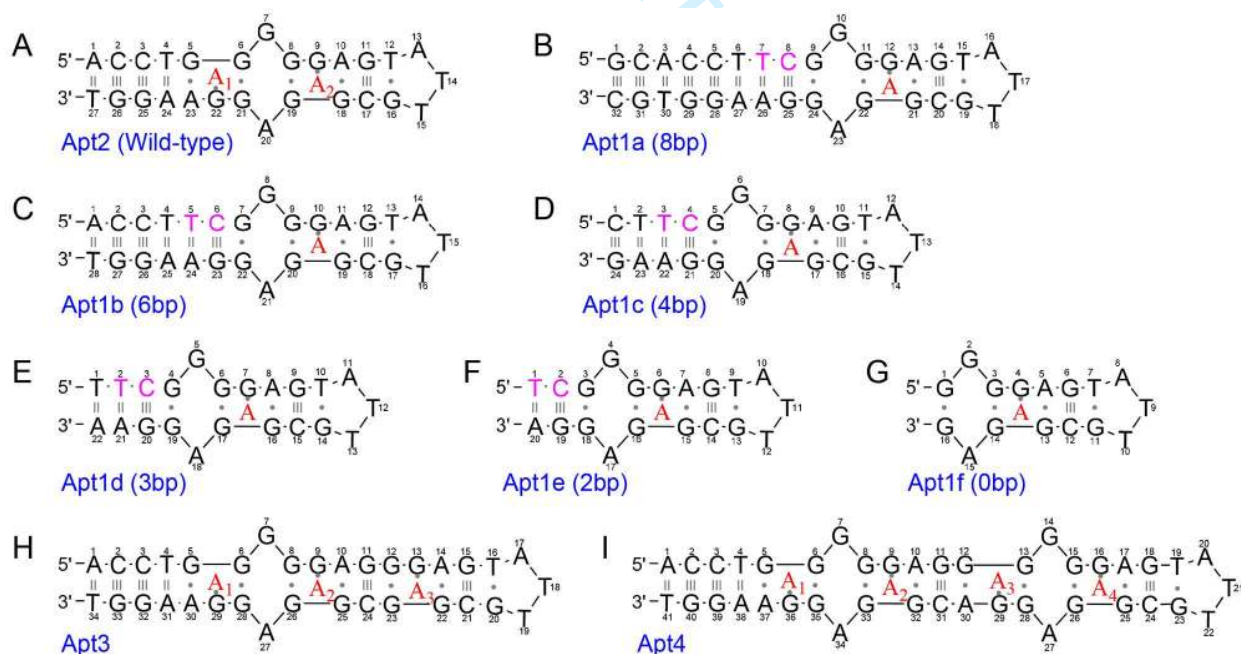
3 **Sensor preparation and test.** Different DNA aptamers (100 nM) were respectively mixed with  
4 an excess concentration of GO (100  $\mu\text{g}/\text{mL}$ ) at 25  $^{\circ}\text{C}$  in the buffer A for 1 h to make sure all the  
5 DNA was adsorbed. No free DNA was left in the buffer solution (confirmed using UV  
6 spectroscopy after centrifugation). The sensors were freshly prepared before each test. The  
7 sensor signaling kinetics were monitored on a Varian Eclipse fluorescence spectrometer with  
8 excitation at 490 nm and emission at 520 nm using 4  $\mu\text{M}$  (2 $\times$ ) SYBR Green (SG) dye at 25  $^{\circ}\text{C}$  in  
9 buffer A. After monitoring the background for 10 min, different concentrations of adenosine or  
10 other nucleosides and nucleotides were added, followed by another  $\sim 40$  min of monitoring.  
11 Multiple samples of the free sensors without adenosine were measured to calculate the standard  
12 deviation of the background variation ( $\sigma$ ). Then the initial slope of the calibration curve was  
13 calculated to determine the limit of detection ( $3\sigma/\text{slope}$ ). To determine the sensor performance in  
14 biological samples, fresh fetal bovine serum (FBS, 1% v/v) was spiked with different  
15 concentrations of adenosine. The sensor was prepared and tested in the same way as in buffer.

## 16 **Results and Discussion**

17 **Engineered adenosine aptamers with different binding sites.** The secondary structure of the  
18 wild-type adenosine aptamer is shown in Figure 1A. This aptamer is named Apt2, where the '2'  
19 describes its binding to two adenosine molecules based on its NMR structure.<sup>25</sup> To facilitate  
20 discussion, each nucleotide in the aptamer is numbered. The two adenosine binding pockets are  
21 relatively symmetric (the red colored 'A<sub>1</sub>' and 'A<sub>2</sub>' denote for the target adenosine). We recently  
22 found that binding was still retained by deleting a site or adding more sites, as long as the

1 binding pocket could stably form.<sup>26</sup> For example, by inserting an extra cytosine base and fixing  
 2 the G5·A23 mismatch, a one-site aptamer is produced (Figure 1C).

3 Analytically, cooperative binding of multiple analytes can produce a sigmoidal switch-like  
 4 response, while the sensitivity at low analyte concentrations is usually low.<sup>40</sup> Therefore, the one-  
 5 site aptamers are interesting since they might be more sensitive. Our main focus in this study is  
 6 to systematically study the new one-site aptamers for better analytical applications. The folded  
 7 aptamer has a stem-loop structure. After removing a binding site, the main parameter for  
 8 optimization is the length of the aptamer stem structure. We systematically varied the number of  
 9 base pairs (bp) from 8 to 0 (Figure 1B-G). The aptamers with shorter arms may have different  
 10 binding affinities to GO and to adenosine, thus affecting the analytical performance. For  
 11 comparison, we also designed two aptamers with even more binding sites (Apt3 and Apt4,  
 12 Figure 1H-I).

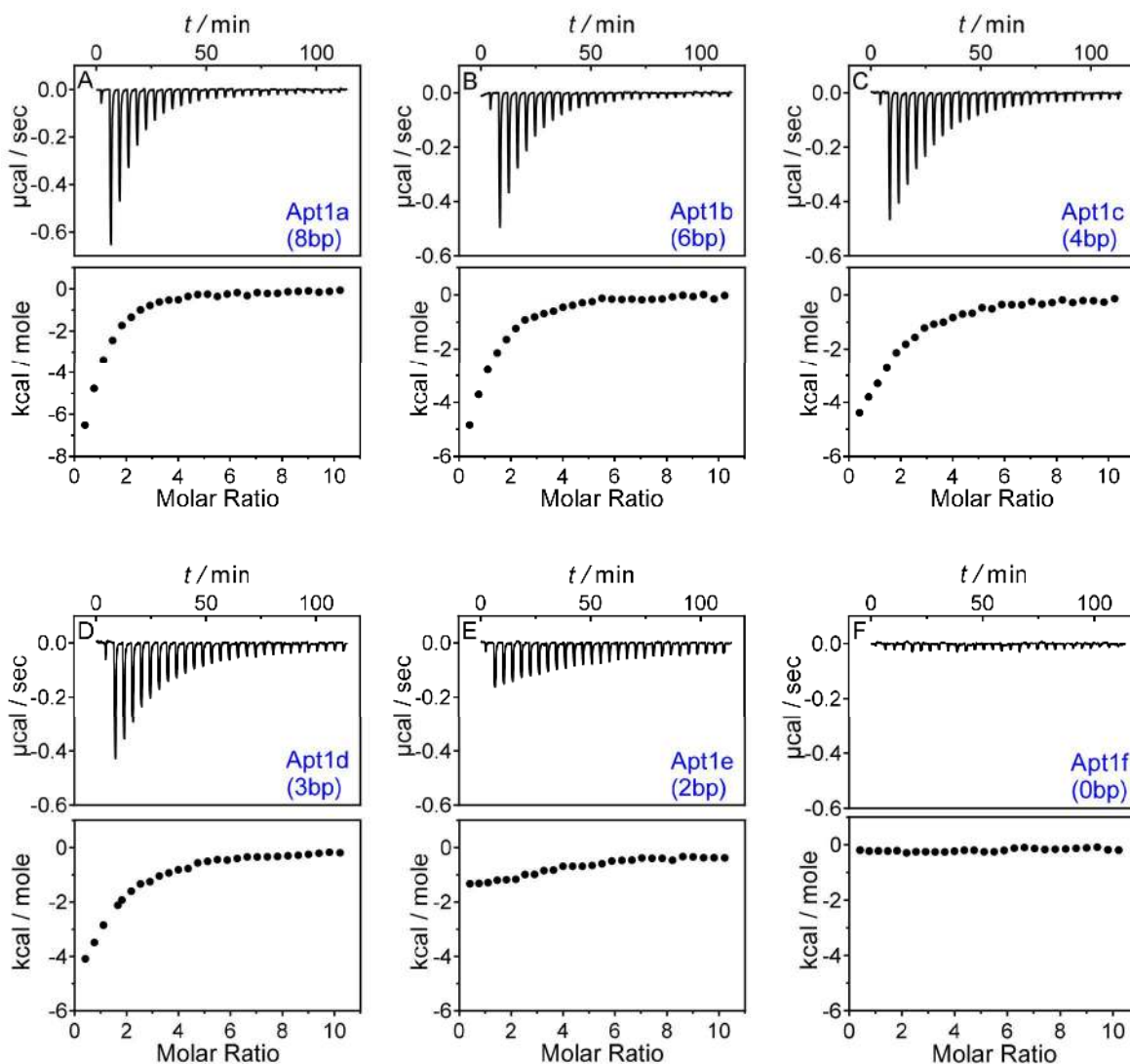


13

1 **Figure 1.** The secondary structures of (A) the wild-type adenosine aptamers (Apt2) with two  
2 adenosine binding sites, (B–G) the engineered one-site aptamers with different stem lengths, and  
3 the extended aptamers with (H) 3 and (I) 4 adenosine binding sites. The wild-type aptamer has  
4 two binding sites ( $A_1$  and  $A_2$ ). The red colored ‘A’ represents the bound adenosine. The  
5 nucleotides in pink were introduced to remove adenosine binding sites. Each nucleotide in the  
6 aptamers is numbered.

7  
8 **Binding thermodynamics measured by ITC.** To confirm binding, we first measured the  
9 binding affinity of the aptamers using isothermal titration calorimetry (ITC). ITC is a label-free  
10 technique providing rich thermodynamic information for aptamer binding.<sup>41-43</sup> Our previous  
11 work has measured the wild-type two-site aptamer (Apt2) and demonstrated that the one-site  
12 mutant has a similar binding affinity.<sup>26</sup> Here we measured the effect of the number of base pairs  
13 in the aptamer stem (Figure 2). In these experiments, adenosine was gradually titrated into the  
14 aptamer solution, and the downward spikes indicate heat release and binding. The aptamers  
15 Apt1a to Apt1d (Figure 2A-D) with more than 3 bp in the stem showed a significant heat release  
16 indicating strong binding. However, further shortening the aptamer (e.g. Apt1e and Apt1f) to 2  
17 or 0 bp nearly fully inhibited binding (Figure 2E and F). By observing the trend, it appears that a  
18 longer stem resulted in a tighter binding of adenosine.





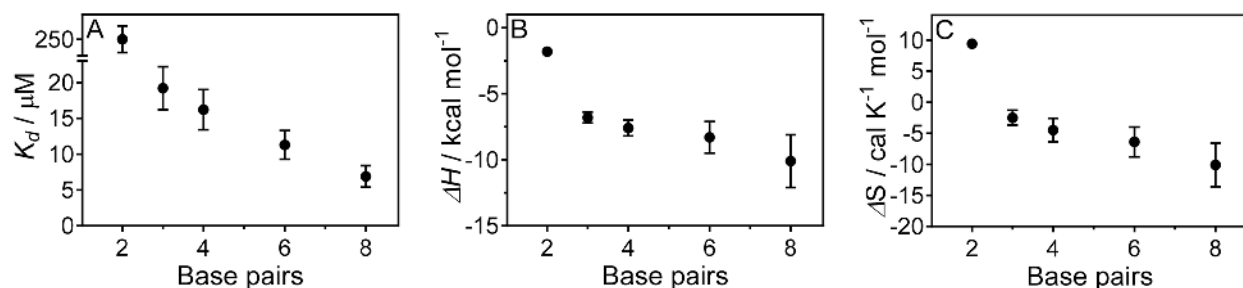
1  
2 **Figure 2.** ITC traced and integrated the heat of the one-site aptamers with various base pairs in  
3 the stem region of the aptamers. In each figure, the top panel is the original thermogram and the  
4 bottom panel is the integrated heat.

5  
6 For quantitative analysis, we integrated the heat of each titration (Figure 2, lower panels) to  
7 directly obtain the reaction enthalpy ( $\Delta H$ ), binding stoichiometry ( $n$ ) and dissociation constant  
8 ( $K_d$ ), which allowed further calculation of  $\Delta G$  and  $\Delta S$ .<sup>44-46</sup> We first compared the aptamers'

1 binding affinity using the  $K_d$  values as a function of the number of base pairs in the stem (Figure  
2 3A). The Apt1a aptamer with the longest stem (8 bp) showed the lowest  $K_d$  ( $7.1 \pm 1.2 \mu\text{M}$ )  
3 indicating the tightest binding. As the base pairs reduced from 8 to 0 (Apt1b to Apt1e), the  
4 aptamers' binding affinity gradually decreased. We reason that longer stems provide a more  
5 stable aptamer structure and result in tighter binding. All the aptamers with more than 3 bp  
6 (Apt1a to Apt1d) retained a high binding affinity ( $K_d \sim 7.1$  to  $19.2 \mu\text{M}$ ). However, the Apt1e  
7 with only two base pairs showed very poor binding ( $K_d > 250 \mu\text{M}$ ) and the even shorter Apt1f  
8 lost all its binding activity. All the thermodynamic parameters are tabulated in Table S1  
9 (Supplementary Data).

10 We also compared the enthalpy changes ( $\Delta H$ ) and entropy changes ( $\Delta S$ ) in these aptamers. All  
11 the binding aptamers released heat (Figure 3B), but showed decreased entropy change (Figure  
12 3C) upon binding to adenosine. The trend of enthalpy change matched well with that of in  $K_d$ .  
13 Therefore, binding was mainly driven by enthalpy.<sup>47,48</sup> From these results we concluded that all  
14 the one-site aptamers with more than 3 bp can bind adenosine, and longer stems resulted in  
15 tighter binding. The Apt1d with 3 base pairs is the limit that has the shortest sequences while still  
16 retaining a relatively high affinity.

17



18

1 **Figure 3.** The (A) dissociation constant ( $K_d$ ), (B) enthalpy change ( $\Delta H$ ), and (C) entropy change  
2 ( $\Delta S$ ) of the one-site adenosine aptamers as a function of the number of base pairs in the stem  
3 region.

4  
5 **Sensitivity as a function of binding sites.** After measuring the binding of our engineered one-  
6 site aptamers, we next used them for designing biosensors. Graphene oxide (GO) was used as a  
7 platform for DNA aptamer adsorption.<sup>33-35</sup> The GO sheets were negative charged ( $\zeta$ -potential: -  
8  $42.1 \pm 5.6$  mV) with an average size around 820 nm measured by DLS and TEM (Figure S1 and  
9 S2). By adding adenosine, the aptamers can bind the target molecule and the equilibrium is  
10 shifted towards desorption from GO (Figure 4A).<sup>31,49</sup> To detect the signal, we used SYBR Green  
11 I to stain the released DNA aptamers for fluorescence output.<sup>50,51</sup> This label-free method is  
12 attractive for its simplicity and cost-effectiveness.<sup>52-56</sup>

13 The sensor performance was evaluated by measuring the signaling kinetics. To ensure all the  
14 DNA aptamers were adsorbed, extra GO (100  $\mu\text{g/mL}$ ) was used for DNA adsorption in a high  
15 salt buffer condition (buffer A: 20 mM HEPES, pH 7.6, 100 mM NaCl, 2 mM  $\text{MgCl}_2$ ).<sup>34</sup> Full  
16 adsorption was confirmed by UV-vis spectroscopy. Using the wild-type aptamer (Apt2) as an  
17 example, we monitored the background fluorescence of the aptamer/GO complex mixed with SG  
18 for 10 min and the signal remained stable (Figure 4C). Then 1 mM adenosine was quickly added  
19 (the arrowhead), and an immediate fluorescence increase was observed. It took around 10 min  
20 for the fluorescence signal to reach saturation and then the signal remained stable for a long time,  
21 indicating that the system reached equilibrium.

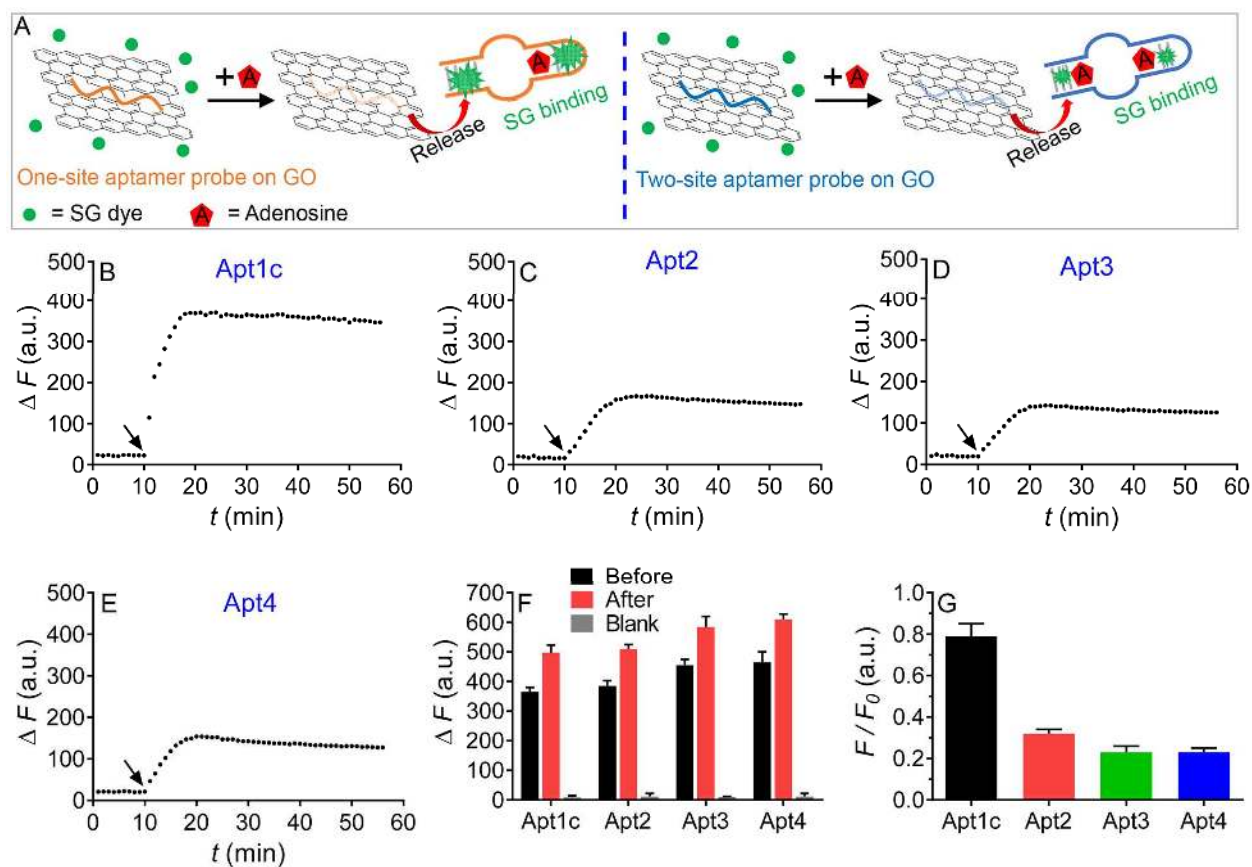
1 Using this method, we then compared the sensor performance of the aptamers with different  
2 numbers of binding sites (Figure 4B-E). These aptamers included the one-site (Apt1c), two-site  
3 (Apt2), three-site (Apt3) and four-site (Apt4), and all these four aptamers had the same stem  
4 length (4 bp, see the structures in Figure 1). Among them, the engineered one-site aptamer had  
5 the best performance (Figure 4B). It showed a similar background as the wild-type aptamer,  
6 while the final signal was more than two-fold higher.

7 Since each aptamer has a different length, they may have a different final fluorescence after  
8 binding adenosine. To understand the effect of DNA length, we also measured the fluorescence  
9 intensity of the free aptamers without GO (Figure 4F). While SG is strongly fluorescent upon  
10 binding to double-stranded DNA, it is also fluorescent with a high concentration of single-  
11 stranded DNA.<sup>50</sup> The three- and four- sites aptamers (Apt3 and Apt4) had a slightly higher  
12 fluorescence likely due to their longer sequences than the Apt1c and Apt2 (Figure 1). After  
13 adding adenosine, the relative fluorescence increase of each aptamer was around 20-30%.  
14 Therefore, without GO, SG is not very effective in sensing the binding of adenosine.

15 With each free aptamers' intensity ( $F_0$ , Figure 4F the red bars) and their maximum released  
16 fluorescence ( $F$ , Figure 4B-E), we normalized each aptamers' fluorescent signaling ( $F/F_0$ , Figure  
17 4G). This ratio has taken the fluorescence difference due to DNA length change into  
18 consideration, and thus is a pure indication of the relative amount of DNA released from GO due  
19 to binding to adenosine. Among the different aptamers, the one-site aptamer Apt1c had the  
20 highest ratio at approximately 0.76 (i.e. 76% aptamer desorbed from GO), which was more than  
21 2.5-fold higher than the multiple-site aptamers (Figure 4G).

22 It is known that all the binding sites have a similar binding affinity,<sup>26</sup> and thus the higher  
23 sensitivity of the one-site aptamer on GO was due to its fewer binding sites. Note the signaling

1 efficiency was quite similar for the free aptamers (without GO) (Figure 4F). GO improved the  
 2 signaling for all the aptamers and the most improvement was seen with the one-site aptamer.  
 3 Since an aptamer needs to form a full binding complex to leave the GO surface, the multi-site  
 4 aptamers are more difficult to satisfy this requirement and thus they require higher adenosine  
 5 concentrations.



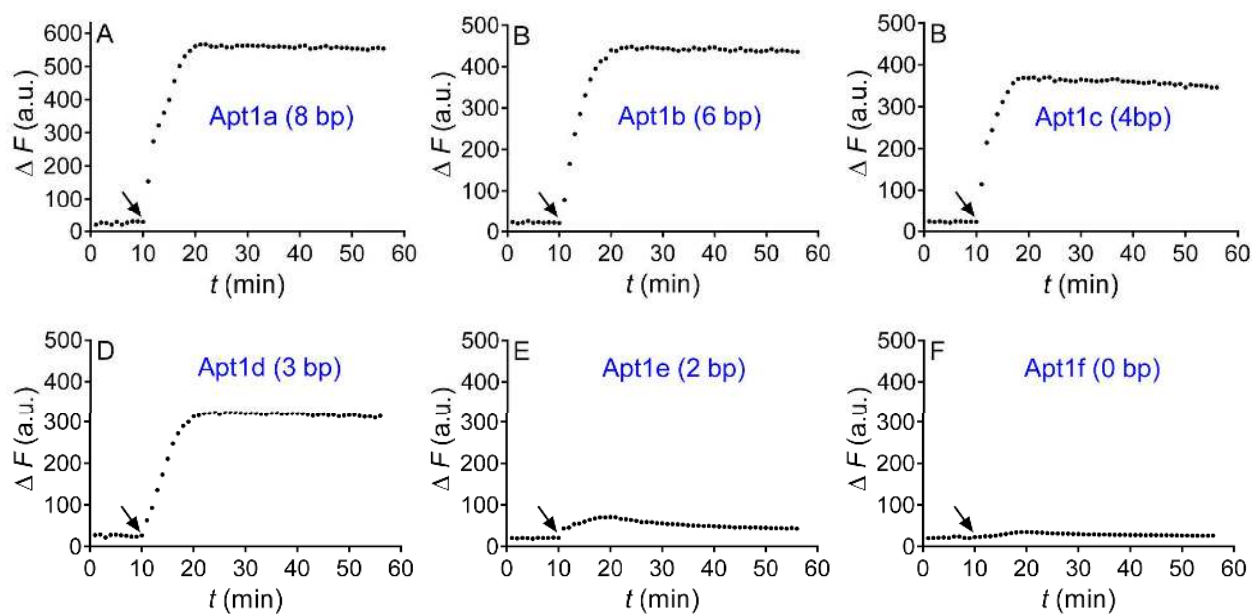
6  
 7 **Figure 4.** (A) Schemes of the designed sensors with label-free fluorescence signaling, showing  
 8 the one-site aptamer is more sensitive. Fluorescence signaling kinetics of the adenosine aptamers  
 9 with different numbers of binding sites: (B) Apt1c, (C) Apt2, (D) Apt3, and (E) Apt4 released  
 10 from GO (100  $\mu\text{g/mL}$ ) tested at 25  $^{\circ}\text{C}$  in the buffer A. 1 mM of adenosine were added in 10 min  
 11 (pointed by the arrowheads). (F) Fluorescence intensities of the free aptamers stained by SG  
 12 before and after adding 1 mM adenosine. The Blank control was the intensity of SG with

1 adenosine but without any DNA. (G) The normalized fluorescence ratio of the aptamers with GO  
2 over that without GO ( $F/F_0$ ). The chemical meaning is the fraction of aptamers released from the  
3 GO surface. All the aptamers were 100 nM, and the SG was 4  $\mu$ M (2 $\times$ ).

4  
5 **Sensitivity as a function of stem length.** After confirming that the one-site aptamer had the best  
6 performance, we then further studied the effect of the stem length. We tested a series of one-site  
7 aptamers with various base pairs (0 to 8 bps, see Figure 1) in the same way. We first measured  
8 their signaling kinetics. The Apt1a with the longest 8 bp stem showed the highest final  
9 fluorescence intensity (Figure 5A). By shortening the stem, the final intensities gradually became  
10 lower (Figure 5B-F). This difference may be related to either the aptamers' binding affinities  
11 according to the ITC results, or the fluorescence of the free aptamers after stained by SG, or both.  
12 To identify the reason, we measured the signaling of the free aptamers (Figure 6A). It is very  
13 interesting to note that the fluorescence of the free aptamers was roughly linearly correlated with  
14 the length of the aptamers. This is not surprising since longer DNA produces more signals with  
15 SG staining. Adenosine barely induced any fluorescence change for the very short 0 and 2 bp  
16 aptamers, while the signal increase by adenosine was similar (around 20%) for all the longer  
17 aptamers.

18 We then calculated the fluorescence ratios with and without GO as we did above ( $F/F_0$ , Figure  
19 6B) which is roughly the fraction of aptamer released from GO. Among the aptamers, the ones  
20 with more than 3 bp all had a high and similar efficiency of  $\sim 0.81$ , indicating their similar and  
21 excellent sensor performance (Figure 6B). We reason that longer aptamers bind adenosine more  
22 tightly according to ITC but they also bind to GO more tightly. Therefore, these two factors  
23 cancelled out with each other, leading to a similar desorption ratio. From the signaling standpoint

1 in the current system, the aptamers with a longer stem are still better due to the very low  
2 background fluorescence. The aptamers with less than 2 bp showed a much lower fraction of  
3 release which was consistent with their loss of adenosine binding from our ITC data (Figure 3A).  
4 When comparing with two- and multiple-site aptamers, all the one site aptamers with more than  
5 3 bp had better sensing performance with an efficiency of  $\sim 0.8$  (Figure 6B), which is more than  
6 two-fold higher than that of the two- and multiple-site aptamers ( $\sim 0.3$ , Figure 4G). From these  
7 tests, we concluded that all the one-site aptamers with more than 3 bp in the stem had better  
8 biosensor performance than the wild-type two-site aptamer.



9  
10 **Figure 5.** Fluorescence signaling kinetics of one-site adenosine aptamers with various stem  
11 lengths adsorbed on GO (100  $\mu\text{g}/\text{mL}$ ) tested at 25  $^{\circ}\text{C}$  in the buffer A. 1 mM of adenosine were  
12 added at 10 min. 4  $\mu\text{M}$  SG was used in all the tests.

13

1 **Highly sensitive label-free detection.** Since the one-site aptamers with 3-8 bp stems all showed  
2 a similar performance and shorter aptamers are more cost effective, we next chose the Apt1d  
3 with 3 bp for biosensor tests. Compared to the wild-type 27 nucleotide aptamer, this 3 bp  
4 aptamer has only 22 nucleotides. To quantitatively evaluate the sensor performance, we  
5 gradually titrated adenosine to the Apt1d sensor and a comparison was also made with the wild-  
6 type Apt2 sensor (Figure 6C). Both sensors followed a linear growth trend initially, with a slope  
7 of  $235 \pm 19$  (a.u./mM) for Apt1d, and  $56 \pm 6$  (a.u./mM) for Apt2. Then, we calculated the limit  
8 of detection (LOD) of Apt1d to be  $12.8 \mu\text{M}$  adenosine, which was 4.2-fold better than that of  
9 Apt2 with ( $53.9 \mu\text{M}$ , Figure 6C). The LOD was calculated based on the adenosine concentration  
10 at which the signal was three times higher than background variation.

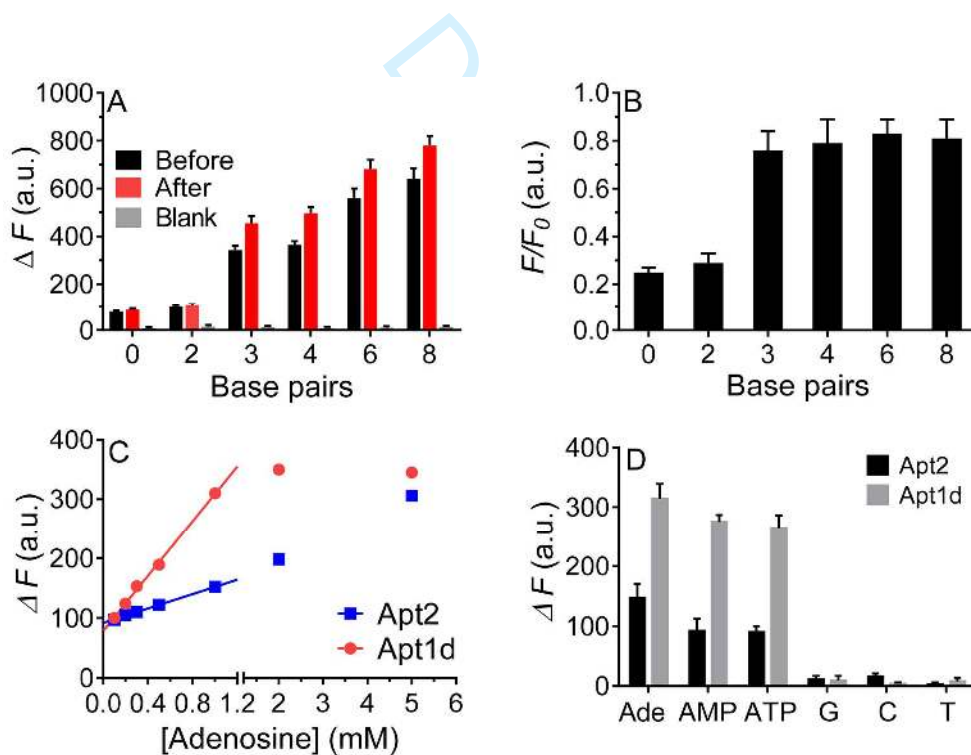
11 We also tested the specificity of the two sensors by adding AMP, ATP and other nucleosides  
12 such as guanosine (G), cytidine (C), thymidine (T) (Figure 6D). Regardless of AMP or ATP, the  
13 sensor with the one-site Apt1d aptamer showed stronger intensity than that with the two-site  
14 Apt2 aptamer. Overall, adenosine had the highest sensitivity among these tested derivatives, and  
15 this is consistent with the literature reports.<sup>15,57,58</sup> On the other hand, both sensors showed almost  
16 no response to other nucleosides confirming excellent specificity for adenosine and its  
17 derivatives (Figure 6D).

18 Aptamer/GO based sensors used for ATP/adenosine detection have been a widely studied model  
19 system. We summarized different sensing methods in recent years in the Table S2. Aptamers  
20 with a covalently labeled fluorophore is one of most used strategies. While it is easy to operate,  
21 label-free sensors have also been explored for cost-effectiveness. Such covalent sensors have a  
22 detection limit of a few micromolar. With signal amplification methods, such as using  
23 exonuclease or other enzymes, much lower detection limits of low nanomolar was possible.



1 However, such sensing methods take longer time and are more difficult to control. Label-free  
 2 sensors are around 10  $\mu\text{M}$  detect limit. Adenosine in normal cells are approximately 0.3  $\mu\text{M}$  and  
 3 elevate to 1.2  $\mu\text{M}$  in response to cellular damage. Most adenosine are converted to adenosine  
 4 triphosphate (ATP) which has an abundant concentration of 1–10 mM.<sup>59</sup> This aptamer is known  
 5 to bind adenosine, AMP and ATP with quite similar  $K_d$ 's. Therefore, it is likely useful for ATP  
 6 measurement for intracellular applications. We here used adenosine as a more cost-effective  
 7 alternative. The main goal of this work is to study the analytical performance of the shortened  
 8 one-site aptamer, which from our side-by-side comparison, was more sensitive than the original  
 9 two-site aptamer.

10

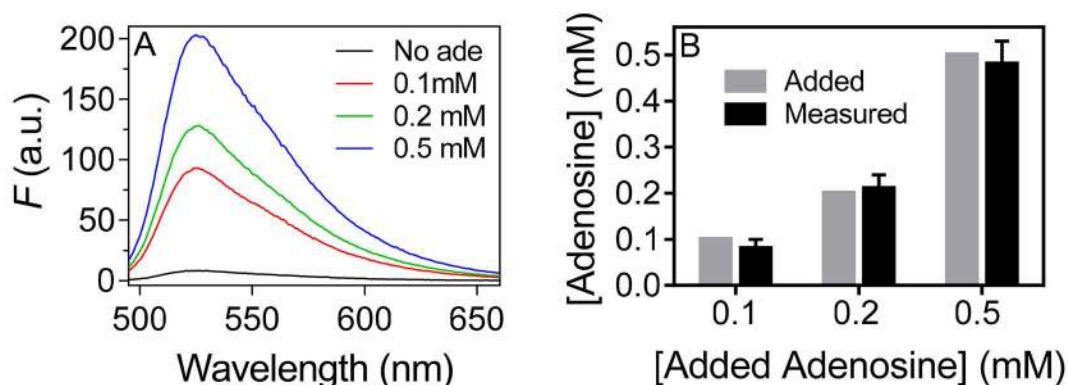


11

12 **Figure 6.** (A) Fluorescence intensity of different free aptamers binding in the presence of SG  
 13 before and after adding 1 mM adenosine. The blank control is the intensity of SG with adenosine  
 14 but without aptamers. (B) The fluorescent signaling efficiency ( $F/F_0$ ) of the one-site aptamers

1 with different base pairs released from GO. (C) The fluorescence intensity of the two sensors  
2 using Apt2 and Apt1d after 40 min as a function of adenosine concentration. (D) Fluorescence  
3 intensity of the two sensors using Apt2 and Apt1d (one site, 3 bps) by adding 1 mM of different  
4 nucleotide or nucleosides measured in 40 min. All the used aptamers were 100 nM. 4  $\mu$ M SG  
5 was used in all the tests at 25 °C in the buffer A.

6 **Detection of adenosine in serum samples.** To test whether this sensor is capable of measuring  
7 adenosine in biological samples, we then applied the Apt1d-GO sensor in the presence of fetal  
8 bovine serum (FBS). Three serum samples with different concentrations of spiked adenosine (0.1,  
9 0.2 and 0.5 mM) were tested (all within the linear calibration range in Figure 6C). The sensor  
10 showed weak fluorescence in the adenosine-free sample (Figure 7A, black curve) but strong  
11 intensity in adenosine-containing samples (Figure 7A), which confirmed the sensor performance  
12 in serum. With the calibration curve, the adenosine in these samples were measured (Figure 7B,  
13 grey bars), which were all close to the added concentrations (Figure 7B, black bars) with an  
14 average recovery rate of 93.6 %.



15  
16 **Figure 7.** (A) Fluorescence emission spectra of Apt1d-GO sensors tested in adenosine-free (No  
17 ade), and a few adenosine containing (0.1-0.5 mM) serum samples (1%). (B) The concentration  
18 of adenosine added in three serum samples and measured by the GO-Apt1d sensors.

1

## 2 **Conclusions**

3 In this study, we focused our attention on our newly discovered one-site aptamers binding  
4 adenosine. The original adenosine aptamer has two binding sites, which is quite unique among  
5 the in vitro selected small molecule binding aptamers. By rationally designing the sequence, we  
6 removed one of the binding sites and studied the one-site aptamer using ITC and a label-free  
7 fluorescence signaling method. The one-site aptamer, although it has a similar binding affinity,  
8 showed much better sensitivity on the GO sensing platform. We further measured the effect of  
9 the length of the stem region of the one-site aptamer, and found that aptamers with more than 3  
10 base pairs showed similar sensitivity. This allowed us to shorten the original 27-mer aptamer to  
11 22-mer, while still retaining a high sensitivity (4.2-fold lower LOD than the sensor with the two-  
12 site aptamer). Furthermore, the sensor is also capable of measuring adenosine in biological  
13 samples with a recovery rate of 93.6 %. This work has provided a series of aptamers based on  
14 this highly important model adenosine aptamer system for biosensor development, and it has  
15 demonstrated the relationship between the number of binding sites, sensitivity, and signal  
16 intensity.

## 17 **Acknowledgement**

18 Funding for this work was from The Natural Sciences and Engineering Research Council of  
19 Canada (NSERC).

## 20 **References:**

- 21 (1) Tuerk, C.; Gold, L. *Science* **1990**, *249*, 505.  
22 (2) Ellington, A. D.; Szostak, J. W. *Nature* **1990**, *346*, 818.

- 1 (3) Winkler, W.; Nahvi, A.; Breaker, R. R. *Nature* **2002**, *419*, 952.
- 2 (4) Liu, J.; Cao, Z.; Lu, Y. *Chem. Rev.* **2009**, *109*, 1948.
- 3 (5) Li, D.; Song, S. P.; Fan, C. H. *Acc. Chem. Res.* **2010**, *43*, 631.
- 4 (6) Tan, W. H.; Donovan, M. J.; Jiang, J. H. *Chem. Rev.* **2013**, *113*, 2842.
- 5 (7) Zhao, W.; Brook, M. A.; Li, Y. *ChemBioChem* **2008**, *9*, 2363.
- 6 (8) Zhang, H.; Li, F.; Dever, B.; Li, X.-F.; Le, X. C. *Chem. Rev.* **2013**, *113*, 2812.
- 7 (9) Wilner, O. I.; Willner, I. *Chem. Rev.* **2012**, *112*, 2528.
- 8 (10) Cho, E. J.; Lee, J.-W.; Ellington, A. D. *Annu. Rev. Anal. Chem.* **2009**, *2*, 241.
- 9 (11) Xiang, Y.; Lu, Y. *Inorg. Chem.* **2014**, *53*, 1925.
- 10 (12) Zhou, W.; Saran, R.; Liu, J. *Chem. Rev.* **2017**.
- 11 (13) Winkler, W. C.; Breaker, R. R. *Annu. Rev. Microbiol.* **2005**, *59*, 487.
- 12 (14) Liu, J.; Lu, Y. *Angew. Chem., Int. Ed.* **2006**, *45*, 90.
- 13 (15) Huizenga, D. E.; Szostak, J. W. *Biochemistry* **1995**, *34*, 656.
- 14 (16) Zheng, D.; Seferos, D. S.; Giljohann, D. A.; Patel, P. C.; Mirkin, C. A. *Nano Lett.*  
15 **2009**, *9*, 3258.
- 16 (17) Nutiu, R.; Li, Y. *J. Am. Chem. Soc.* **2003**, *125*, 4771.
- 17 (18) Liu, J.; Lu, Y. *Angew. Chem.* **2006**, *118*, 96.
- 18 (19) Wang, Y.; Li, Z.; Hu, D.; Lin, C.-T.; Li, J.; Lin, Y. *J. Am. Chem. Soc.* **2010**, *132*,  
19 9274.
- 20 (20) Zhang, Z.; Liu, J. *ACS Appl. Mater. Inter.* **2016**, *8*, 6371.
- 21 (21) Li, L.-L.; Ge, P.; Selvin, P. R.; Lu, Y. *Anal. Chem.* **2012**, *84*, 7852.
- 22 (22) Meng, H.-M.; Zhang, X.; Lv, Y.; Zhao, Z.; Wang, N.-N.; Fu, T.; Fan, H.; Liang,  
23 H.; Qiu, L.; Zhu, G.; Tan, W. *ACS Nano* **2014**, *8*, 6171.

- 1 (23) Hermann, T.; Patel, D. J. *Science* **2000**, *287*, 820.
- 2 (24) Sassanfar, M.; Szostak, J. W. *Nature* **1993**, *364*, 550.
- 3 (25) Lin, C. H.; Patel, D. J. *Chem. Biol.* **1997**, *4*, 817.
- 4 (26) Zhang, Z.; Oni, O.; Liu, J. *Nucleic Acids Res.* **2017**.
- 5 (27) He, S.; Song, B.; Li, D.; Zhu, C.; Qi, W.; Wen, Y.; Wang, L.; Song, S.; Fang, H.;  
6 Fan, C. *Adv. Func. Mater.* **2010**, *20*, 453.
- 7 (28) Liu, Z.; Liu, B.; Ding, J.; Liu, J. *Anal. Bioanal. Chem.* **2014**, *406*, 6885.
- 8 (29) Chen, D.; Feng, H.; Li, J. *Chem. Rev.* **2012**, *112*, 6027.
- 9 (30) Wang, H.; Yang, R.; Yang, L.; Tan, W. *ACS Nano* **2009**, *3*, 2451.
- 10 (31) Lu, C. H.; Yang, H. H.; Zhu, C. L.; Chen, X.; Chen, G. N. *Angew. Chem. Int. Ed.*  
11 **2009**, *121*, 4879.
- 12 (32) Liu, Y.; Yu, D.; Zeng, C.; Miao, Z.; Dai, L. *Langmuir* **2010**, *26*, 6158.
- 13 (33) Lee, J.; Yim, Y.; Kim, S.; Choi, M.-H.; Choi, B.-S.; Lee, Y.; Min, D.-H. *Carbon*  
14 **2016**, *97*, 92.
- 15 (34) Liu, B.; Salgado, S.; Maheshwari, V.; Liu, J. *Curr. Opin. Colloid Interface Sci.*  
16 **2016**, *26*, 41.
- 17 (35) Lu, C.; Huang, Z.; Liu, B.; Liu, Y.; Ying, Y.; Liu, J. *Angew. Chem. Int. Ed.* **2017**,  
18 *56*, 6208.
- 19 (36) Wu, M.; Kempaiah, R.; Huang, P.-J. J.; Maheshwari, V.; Liu, J. *Langmuir* **2011**,  
20 *27*, 2731.
- 21 (37) Li, J.; Huang, Y.; Wang, D.; Song, B.; Li, Z.; Song, S.; Wang, L.; Jiang, B.; Zhao,  
22 X.; Yan, J. *Chem. Commun.* **2013**, *49*, 3125.

- 1 (38) Jiang, Y.; Tian, J.; Chen, S.; Zhao, Y.; Wang, Y.; Zhao, S. *J. Fluorescence* **2013**,  
2 23, 697.
- 3 (39) Zhang, Y.; Liu, Y.; Zhen, S. J.; Huang, C. Z. *Chem. Commun.* **2011**, 47, 11718.
- 4 (40) Simon, A. J.; Vallée-Bélisle, A.; Ricci, F.; Watkins, H. M.; Plaxco, K. W. *Angew.*  
5 *Chem. Int. Ed.* **2014**, 126, 9625.
- 6 (41) Turnbull, W. B.; Daranas, A. H. *J. Am. Chem. Soc.* **2003**, 125, 14859.
- 7 (42) Ghai, R.; Falconer, R. J.; Collins, B. M. *J. Mol. Recognit.* **2012**, 25, 32.
- 8 (43) Zhang, Z.; Zhang, X.; Liu, B.; Liu, J. *J. Am. Chem. Soc.* **2017**, 139, 5412.
- 9 (44) Wiseman, T.; Williston, S.; Brandts, J. F.; Lin, L.-N. *Anal. Biochem.* **1989**, 179,  
10 131.
- 11 (45) Lin, P.-H.; Chen, R.-H.; Lee, C.-H.; Chang, Y.; Chen, C.-S.; Chen, W.-  
12 Y. *Colloids Surf. B* **2011**, 88, 552.
- 13 (46) Zhang, Z.; Liu, B.; Liu, J. *Small* **2016**, 1602730.
- 14 (47) Kimoto, M.; Yamashige, R.; Matsunaga, K.-i.; Yokoyama, S.; Hirao, I. *Nat.*  
15 *Biotechnol.* **2013**, 31, 453.
- 16 (48) Neves, M. A.; Slavkovic, S.; Churcher, Z. R.; Johnson, P. E. *Nucleic Acids Res.*  
17 **2017**, 45, 1041.
- 18 (49) Liu, B.; Sun, Z.; Zhang, X.; Liu, J. *Anal. Chem.* **2013**, 85, 7987.
- 19 (50) Dave, N.; Chan, M. Y.; Huang, P.-J. J.; Smith, B. D.; Liu, J. *J. Am. Chem. Soc.*  
20 **2010**, 132, 12668.
- 21 (51) Wang, J.; Liu, B. *Chem. Commun.* **2008**, 4759.
- 22 (52) Kong, L.; Xu, J.; Xu, Y.; Xiang, Y.; Yuan, R.; Chai, Y. *Biosens. Bioelectron.*  
23 **2013**, 42, 193.

- 1 (53) Wang, Y.; Liu, B. *Analyst* **2008**, *133*, 1593.
- 2 (54) Xu, Y.; Xu, J.; Xiang, Y.; Yuan, R.; Chai, Y. *Biosens. Bioelectron.* **2014**, *51*, 293.
- 3 (55) He, H.-Z.; Ma, V. P.-Y.; Leung, K.-H.; Chan, D. S.-H.; Yang, H.; Cheng, Z.;  
4 Leung, C.-H.; Ma, D.-L. *Analyst* **2012**, *137*, 1538.
- 5 (56) Xiang, Y.; Tong, A.; Lu, Y. *J. Am. Chem. Soc.* **2009**, *131*, 15352.
- 6 (57) Zuo, X.; Song, S.; Zhang, J.; Pan, D.; Wang, L.; Fan, C. *J. Am. Chem. Soc.* **2007**,  
7 *129*, 1042.
- 8 (58) Baaske, P.; Wienken, C. J.; Reineck, P.; Duhr, S.; Braun, D. *Angew. Chem. Int.*  
9 *Ed.* **2010**, *49*, 2238.
- 10 (59) Beis, I.; Newsholme, E. A. *Biochem. J.* **1975**, *152*, 23.

11  
12

13 For Table of Content Graphics Only

